Experimental demonstration of XPM compensation for WDM fibre transmission

L. Zhu, F. Yaman and G. Li

Distributed compensation for cross-phase modulation (XPM) by solving the coupled nonlinear Schrödinger equations in digital backward propagation is demonstrated experimentally. The results show that XPM compensation provides significant improvement over self-phase modulation compensation.

Introduction: Coherent detection combined with digital signal processing is emerging as one of the most promising techniques for long-haul fibre transmission. One of the benefits of coherent detection is that the complete information of the optical field including amplitude and phase can be obtained, which enables the compensation of dispersion and nonlinearity by digital backward propagation [1, 2].

Digital backward propagation (DBP) can be implemented by solving the total-field nonlinear Schrödinger equation (NLSE) or the coupled NLSEs. By solving the coupled NLSEs, cross-phase modulation (XPM) can be compensated while neglecting the effects of four-wave mixing (FWM). In comparison with XPM + FWM compensation by solving the total-field NLSE, XPM compensation via coupled NLSEs requires a smaller computational load [3]. Moreover, XPM compensation does not need phase-locked local oscillators to reconstruct the total optical field. Distributed nonlinearity and dispersion compensation by solving the total-field NLSE has been experimentally demonstrated [4]. In this Letter, we experimentally demonstrate XPM compensation via coupled NLSEs for WDM transmission.

Digital backward propagation: In a coherent wavelength-division multiplexed (WDM) system, the total received field can be expressed as $E = \sum_{m=1}^{N} \hat{E}_m \exp(i2m\pi\Delta f t)$, where $m = \{1, 2, \cdots, N\}$ and N is the total number of channels, $\hat{E}_m$ is the field envelope detected by the coherent receiver for the mth channel, Δf is the channel spacing. The total-field NLSE for backward propagation is given by

$$-\frac{\partial E}{\partial z} + \frac{\alpha}{2}E + \frac{i\beta_2}{2}\frac{\partial^2 E}{\partial t^2} - i\gamma|E|^2 E = 0 \tag{1}$$

where α is the fibre loss, β_2 is the group velocity dispersion, and γ is the nonlinearity parameter [5]. Equation (1) governs the total-field backward propagation where dispersion, self-phase modulation (SPM), XPM and FWM are compensated.

By expanding E in (1) and neglecting the terms for FWM, a set of coupled equations for backward propagation can be derived as [3]

$$\begin{aligned} &-\frac{\partial \hat{E}_m}{\partial z} + \frac{\alpha}{2}\hat{E}_m + 2m\pi\Delta f\beta_2\frac{\partial \hat{E}_m}{\partial t} + \frac{i\beta_2}{2}\frac{\partial^2 \hat{E}_m}{\partial t^2} \\ &- i\gamma\left(2\sum_{q=1}^{N}|\hat{E}_q|^2 - |\hat{E}_m|^2\right)\hat{E}_m = 0 \end{aligned} \tag{2}$$

It is clear from (2) that changes in the relative phase among the channels do not affect the results of backward propagation. As a result, neglecting FWM alleviates the requirement of phase-locking among the local oscillators.

Experimental setup: The experimental setup of the coherent transmission system is shown in Fig. 1. Three distributed-feedback lasers were used as the WDM carriers. Two QPSK modulators were driven by a pattern generator to modulate the central channel and two side channels. Two RF delay lines were used to align the in-phase (I) and quadrature (Q) inputs of the QPSK modulators. The same data pattern with a pseudorandom bit sequence length of $2^{23} - 1$ was used to modulate all the channels. The data sequence of the central channel and the side channels was decorrelated by an optical delay line. The symbol rate was chosen to be 6 Gsymbols/s so that all three WDM channels could fit within the 24 GHz double-sided bandwidth of the real-time oscilloscope. The channel spacing of the WDM channels was set to be 6.8 GHz which made the three WDM channels nearly orthogonal, resulting in the lowest linear crosstalk.

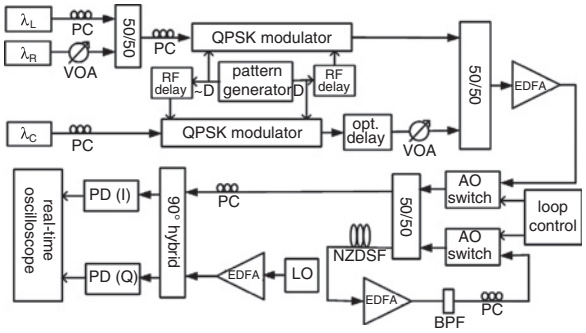

Fig. 1 *Experimental setup of QPSK transmission and coherent detection*

The WDM signal was launched into a recirculating loop controlled by two acousto-optic switches. The length of the nonzero dispersion shifted fibre (NZ-DSF) spool in the loop was 80 km. The total launching power into the fibre was 6 dBm. Variable optical attenuators (VOA) and polarisation controllers (PC) were used to balance the power levels and align the polarisations of the three channels. The local oscillator was tuned to the central channel and mixed with the signal in a 90° hybrid. The I and Q components of the received signal were detected with two photodetectors. The real-time oscilloscope was used for analogue-to-digital conversion at 40 Gsamples/s and data acquisition.

Results: The three WDM channels were demultiplexed using digital filters. Digital backward propagation was performed offline using the split-step Fourier method to solve the coupled NLSEs. Clock recovery, phase estimation and Q-value calculation were performed after compensation of fibre impairments using DBP. The fibre parameters were determined by optimising the performance in the training experiments. The dispersion parameter was found to be 3.9 ps/nm/km by performing dispersion compensation for 80 km transmission. The fibre loss and nonlinear parameter were found to be 0.2 dB/km and 1.4 /W/km by optimising the nonlinearity compensation after 800 km transmission.

In DBP, the step size should be much smaller than the dispersion length $L_D = (\beta_2\Delta\nu^2)^{-1}$ and nonlinear length $L_{NL} = L_{sp}[\gamma P_T \int_0^{L_{sp}} \exp(-\alpha z)dz]^{-1}$, where $\Delta\nu$ is the total bandwidth, L_{SP} is the span length, and P_T is the total launching power. In this system, the dispersion and nonlinear length were 347 km and 675 km, respectively. The Q-value after 640 km transmission and DBP against step size was calculated and shown in Fig. 2. There was no appreciable penalty when the step size was smaller than 80 km. Thus the step size was chosen to be 80 km which was the length of one fibre span.

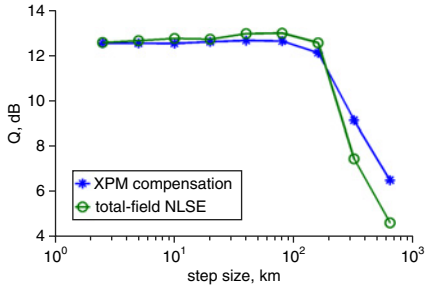

Fig. 2 *Q-value against step size of digital backward propagation*

We used one local oscillator for coherent detection of all the three WDM channels. Therefore, the relative phase among all three channels has been preserved in our measurement. To verify that it is not necessary to preserve the relative phase for XPM compensation, we added random phase shifts (0.1π rad, 1.3π rad and 0.6π rad) to E_1, E_2 and E_3 before solving the coupled NLSEs as expressed in (2). The random phase shifts made no difference to the resulting Q-values.

To evaluate the effectiveness of XPM compensation, other compensation methods are included here for comparison. Fig. 3*a* shows the back-to-back constellation corresponding to a Q-value of 17.6 dB. The constellations after 800 km transmission and digital signal processing are shown in Figs. 3*b–e*. Fig. 3*b* is obtained after dispersion compensation only and the corresponding Q-value is 8.1 dB. Fig. 3*c* is obtained after SPM compensation by neglecting both FWM and XPM terms in the coupled NLSEs and the corresponding Q-value is 8.5 dB. The

constellations after SPM + XPM compensation via coupled NLSEs and nonlinearity compensation via total-field NLSE are shown in Figs. 3*d* and *e*, respectively. The Q-values of the two constellations are both 13.0 dB.

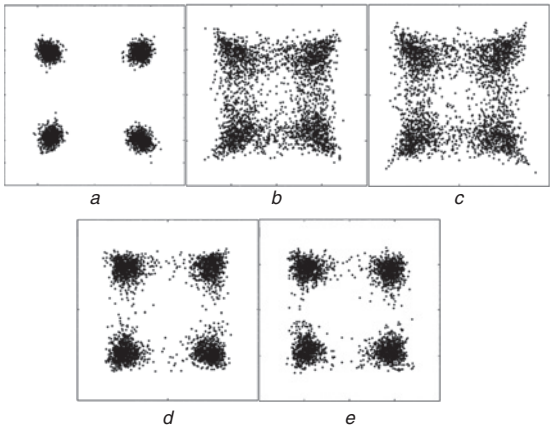

Fig. 3 *Constellations after back-to-back detection (Fig. 3a), dispersion compensation (Fig. 3b), SPM compensation (Fig. 3c), SPM + XPM compensation (Fig. 3d), and nonlinearity compensation via total-field NLSE (Fig. 3e)*

As the transmission distance increases the combined effect of the ASE noise, dispersion and nonlinearity degrades the signal quality further. The dependence of Q-value with transmission distance is shown in Fig. 4. For all transmission distances, the performance improvement due to SPM compensation is negligible but the improvement due to XPM compensation is significant. In this experiment, the performance improvement due to the inclusion of FWM is smaller than what can be expected theoretically [3]. This is due to the fact that FWM components outside the bandwidth of the real-time oscilloscope were not captured for DBP. In addition, FWM compensation via DBP is generally more sensitive to errors in the received waveform.

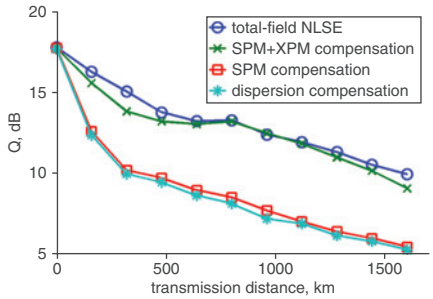

Fig. 4 *Q-value against transmission distance*

Conclusion: XPM compensation using DBP via coupled NLSEs is demonstrated experimentally. Random phase shift is added to the field of each channel verifying that the phase-locking of the local oscillators is not necessary for XPM compensation. The performance of WDM transmission is significantly improved by XPM compensation.

26 May 2010
doi: 10.1049/el.2010.1444
One or more of the Figures in this Letter are available in colour online.

L. Zhu, F. Yaman and G. Li (*CREOL: The College of Optics and Photonics, University of Central Florida, 4000 Central Florida Boulevard, Orlando, FL 32816, USA*)

E-mail: likaizhu@creol.ucf.edu

References

1 Li, X., Chen, X., Goldfarb, G., Mateo, E.F., Kim, I., Yaman, F., and Li, G.: 'Electronic post-compensation of WDM transmission impairments using coherent detection and digital signal processing', *Opt. Express*, 2008, **16**, (2), pp. 880–888
2 Ip, E., and Kahn, J.M.: 'Fiber impairment compensation using coherent detection and digital signal processing', *J. Lightwave Technol.*, 2010, **28**, (4), pp. 502–519
3 Mateo, E.F., and Li, G.: 'Compensation of interchannel nonlinearities using enhanced coupled equations for digital backward propagation', *Appl. Opt.*, 2009, **48**, (25), pp. F6–F10
4 Goldfarb, G., Taylor, M.G., and Li, G.: 'Experimental demonstration of fibre impairment compensation using the split-step finite-impulse-response filtering method', *IEEE Photonics Technol. Lett.*, 2008, **20**, (22), pp. 1887–1889
5 Agrawal, G.P.: 'Nonlinear fibre optics' (Academic Press, 1995, 2nd edn)